Renewable Energy 139 (2019) 688–695

Contents lists available at ScienceDirect

Renewable Energy

journal homepage: www.elsevier.com/locate/renene

Biodiesel production from esterification of oleic acid by a sulfonated magnetic solid acid catalyst

Yi-Tong Wang [a, b, c, *], Xing-Xia Yang [b, c], Jie Xu [a], Hong-Li Wang [a], Zi-Bing Wang [a], Lei Zhang [a], Shao-Long Wang [a], Jing-Long Liang [a, **]

[a] *College of Metallurgy and Energy, North China University of Science and Technology, 21 Bohai Street, Tangshan, 063210, China*
[b] *Biomass Group, Key Laboratory of Tropical Plant Resources and Sustainable Use, Xishuangbanna Tropical Botanical Garden, Chinese Academy of Sciences, 88 Xuefu Road, Kunming, Yunnan Province, 650223, China*
[c] *University of Chinese Academy of Sciences, 19A Yuquan Road, Beijing, 100049, China*

ARTICLE INFO

Article history:
Received 13 April 2018
Received in revised form
19 November 2018
Accepted 20 February 2019
Available online 26 February 2019

Keywords:
Biodiesel
Magnetization
Bronsted and Lewis sites
Esterification

ABSTRACT

Novel sulfonated magnetic solid acid catalysts (ZrFe-SA-SO_3H) with both Bronsted and Lewis sites were synthesized, which provided both a high density of surface acidity (4.4–8.4 mmol/g) and considerable magnetization (3.7–8.1 Am^2/kg). The synthesized catalysts were characterized by elemental analysis, XRD, ICP-OES, FT-IR, BET, SEM-EDX, TEM, TG-DSC, VSM and Boehm titration. The prepared catalysts were tested in the esterification of oleic acid, with high yields of biodiesel (92.7–99.5%) for the first catalytic cycle at 90 °C for 4 h. A High biodiesel yield of 90.3% was still achieved after five cycles of $Zr_{1.0}Fe_{1.0}$-SA-SO_3H. A similar situation was also observed when using sodium carboxymethylcellulose (CMC) to replace SA during catalyst preparation.

1. Introduction

Biodiesel [fatty acid methyl esters (FAMEs)] [1,2] from the transesterification and esterification reactions of plant, animal and illegal cooking oils with methanol [3] is regarded as an ideal supplement for fossil fuels [4,5], and could benefit the remission and elimination of environmental problems [6–9], such as global warming, haze and environmental pollution [10,11]. Along with the rapid population growth and social development, it receives increasing attentions from scientists in the past few decades [12]. Homogeneous acid [13] and base [14] have good catalytic capabilities on biodiesel production, but poor environmental friendliness due to products separation and wastewater treatment [15]. Heterogeneous catalysts have many advantages such as reuse, high activity, simple separation and environmental friendliness, and can be used as substitutes for homogeneous catalysts [16]. Heterogeneous alkaline catalysts [17,18] can catalyze biodiesel production from raw inedible oils *via* transesterification reaction, but serious saponification occurs because these low-grade feed oils contain certain amounts of free fatty acids (FFAs). So additional pretreatment step is very necessary to convert these FFAs to FAMEs before the practical base-catalyzed transesterification, which normally uses homogeneous or heterogeneous acid as catalyst. In the past few years, reported heterogeneous acid catalysts such as functionalized cellulose-magnetite nanocomposite catalysts [19], sulfated zirconia [20], zeolites [21,22] and Nafion [23] have many problems including low catalytic activity, low thermal stability, prone to deactivation and high cost when using in deacidification pretreatment. For example, synthesized E-260-20-SO_3H and E-P400-2-SO_3H acidic carbonaceous catalysts [24] were used in the esterification of oleic acid at 80 °C for 7 h and 5 h reaction time, which gave high yield of 95.4% and 95.5% over the fresh catalysts, but it decreased remarkably to 82% and 47% after five cycles. Reported Cs-tungstosilicic acid Cs-STA/ZK catalyzed oleic acid esterification with biodiesel yields of 88%, 79%, 67%, 60% and 49% for 1–5 cycles under conditions of 120 °C for 5 h [25]. Amberlyst 35, Amberlyst 36 and a sulfonated polydivinylbenzene (polyDVB-SO_3H) esterified oleic acid with methanol at 120 °C in 8 h obtaining 85%, 86% and 87%, respectively [26]. Poly (1-(4-sulfonate)-butyl-3-vinylimidazolium) phosphotungstate was carried out at 65 °C for 6 h with about 70–80% biodiesel yields for 1–5 cycles [27]. Carbon-

---

* Corresponding author. College of Metallurgy and Energy, North China University of Science and Technology, 21 Bohai Street, Tangshan, 063210, China.
** Corresponding author.
E-mail addresses: wangyt@ncst.edu.cn (Y.-T. Wang), ljl@ncst.edu.cn (J.-L. Liang).

https://doi.org/10.1016/j.renene.2019.02.111

based solid acid catalyst SAC-SCB-08-150 from one-step synthesis of sugarcane bagasse catalyzed the esterification of oleic acid with methanol at 65 °C achieving conversion yield of 85% after 24 h for first cycle. After the third cycle, its catalytic performance remained at 67% [28]. Sulfonated activated carbon esterified oleic acid with ethanol under reaction temperature of 85 °C within 180 min, efficiency of 96% was achieved. Under the same condition for 5 times, efficiencies were 96%, 96%, 97%, 97% and 95%, respectively [29]. These mentioned catalysts had no magnetization, which may bring some difficulties in the separation and recycling of catalysts after reactions.

Here, we reported novelty sulfonated magnetic solid acid catalysts with both Brønsted and Lewis sites synthesized by simply chelation and sulfonation method. The catalysts were used in the catalytic esterification of oleic acid, which could be easily separated and recovered from product mixtures after reactions, while the activity and reuse ability of catalysts seemed adjustable and could be improved through the variation of parameters during catalyst preparation.

2. Experimental

2.1. Materials

$ZrOCl_2 \cdot 8H_2O$ (≥98.0%), $Fe_2(SO_4)_3$ (≥99.7%) with Fe content of 21–23% and sodium alginate [SA; powder, viscosity of 200 ± 20 mPa.s] were bought from Aladdin Industrial Co., Ltd. (Shanghai, China). Dehydrated methanol (≥99.5%), oleic acid (AR, molecular weight of 282.5, acid value of 196.0–204.0 mg KOH/g, about 80% purity for oleic acid, and 20% purity for palmitoleate, stearate, linoleate and other free fatty acids), analytical reagents H_2SO_4 (≥98.0%), and NaOH (≥96%) were from Xilong Chemical Factory Co., Ltd. (Shantou, Guangdong, China). Sodium carboxymethylcellulose [CMC; powder, viscosity of 300–800 mPa.s] was purchased from Shanghai Zhanyun Chemical Co., Ltd. (Shanghai, China). Internal standard heptadecanoic acid methyl ester ($C_{17:\ 0}$) was purchased from Sigma (Shanghai, China), as well as other six methyl esters [linolenate ($C_{18:\ 3}$), linoleate ($C_{18:\ 2}$), oleate ($C_{18:\ 1}$), stearate ($C_{18:\ 0}$), palmitoleate ($C_{16:\ 1}$) and palmitate ($C_{16:\ 0}$)] (≥99.0%). Deionized water was obtained by a water purification system (electrical conductivity of 18.2 MΩ cm, Milli-Q Academic, Merck Millipore, Darmstadt, Germany).

2.2. Sulfonated magnetic solid acid catalysts synthesis

$Zr_{1.0}Fe_{1.0}$-SA-SO_3H and $Zr_{1.0}Fe_{1.0}$-CMC-SO_3H catalysts were synthesized *via* four steps: (1) Fe^{3+} ion chelation, (2) calcination, (3) Zr^{4+} ion chelation and embedding, and (4) sulfonation. Each step donated its special contribution to the activity and reuse of the catalyst: (1) The chelation with Fe^{3+} gave a -$(COO)_3Fe$ structure; (2) The subsequent calcination at 400 °C partially reduced the -$(COO)_3Fe$ structure to Fe_3O_4 (the reduction reaction did not occur below 400 °C), and the Fe_3O_4 was used as a stable magnetic core in this study; (3) The chelation and embedding with Zr^{4+} produced a dense carbon shell with a -$(COO)_4Zr$ structure (Lewis acid site) which was stable in the sulfonation process and provided better protection for the magnetic core from sulfuric acid dissolution during the subsequent sulfonation. Without chelation and embedding with Zr^{4+}, the SA or CMC embedding of the magnetic core and the subsequent sulfonation cannot succeed. (4) During sulfonation, the outside carbon shell was partially carbonized, with new strong Brønsted acid sites created on the carbon skeleton for the esterification of oleic acid.

Under magnetic stirring, SA or CMC solution (200 mL, concentration of 20 g/L) was added drop-wise in 200 mL $Fe_2(SO_4)_3$ solution with different concentrations (0.5, 1.0, and 1.5 mol/L) using an injector and was left to stand for 3 h to yield precipitate at room temperature. The precipitate was filtered, washed with distilled water until a *pH* reaching nearly 7, and then dried at 105 °C (WFO-710, EYELA, Tokyo Rikakikai Co., Ltd., Makati, Philippines) overnight. Dry solid residue was ground, passed through a 40 (<425 μm) or 200 mesh sieve (<75 μm), added to 50 mL $Fe_2(SO_4)_3$ solution with different concentrations of 0.5, 1.0, and 1.5 mol/L [keep the same $Fe_2(SO_4)_3$ concentration as the previous step], and was then left to stand for 3 h at room temperature to load Fe homogeneously again. The obtained solid was washed with distilled water, dried at 105 °C overnight, and named as $Fe_{0.5/1.0/1.5}$-SA or $Fe_{0.5/1.0/1.5}$-CMC (subscript of 0.5, 1.0 and 1.5 meant $Fe_2(SO_4)_3$ solution concentrations). The $Fe_{0.5/1.0/1.5}$-SA or $Fe_{0.5/1.0/1.5}$-CMC was calcined at 400 °C for 2 h in a tubular furnace (SGL-1100, Shanghai Daheng Optics and Fine Mechanics Co., Ltd., Shanghai, China) to produce magnetic $Fe_{0.5/1.0/1.5}$-SA and $Fe_{0.5/1.0/1.5}$-CMC with the heating rate of 1 °C/min and nitrogen flow of 200 mL/min.

For the preparation of $Zr_{0.5/1.0/3.0}Fe_{0.5/1.0/1.5}$-SA-$SO_3H$ and $Zr_{1.0}Fe_{0.5/1.0/1.5}$-CMC-SO_3H, 3 g magnetic $Fe_{0.5/1.0/1.5}$-SA or $Fe_{0.5/1.0/1.5}$-CMC and 200 mL SA or CMC solution were mixed, added dropwise into 200 mL $ZrOCl_2$ solution with concentrations of 0.5, 1.0, and 3.0 mol/L under magnetic stirring, and then left to stand for 3 h to produce a dense carbon shell with a -$(COO)_4Zr$ structure. The yielded precipitate was filtered, washed with distilled water, dried at 105 °C overnight and named as $Zr_{0.5/1.0/3.0}Fe_{0.5/1.0/1.5}$-SA or $Zr_{1.0}/Fe_{0.5/1.0/1.5}$-CMC. About 5 g $Zr_{0.5/1.0/3.0}Fe_{0.5/1.0/1.5}$-SA or $Zr_{1.0}/Fe_{0.5/1.0/1.5}$-CMC particles and 100 mL 98% H_2SO_4 were mixed in a 150 mL serum bottle, and then sulfonated with magnetic stirring at 150 °C for 16 h in an oil bath (HH-SJ4CD, Jintan city Youlian Instrument Research Institute, Zhejiang, China). The obtained particles were washed to neutral with hot water (>80 °C), and then completely dried in a freeze dryer at −47 °C. The dry catalysts were ground, passed through a 200 mesh sieve, and named as $Zr_{0.5/1.0/3.0}Fe_{0.5/1.0/1.5}$-SA-$SO_3H$ and $Zr_{1.0}Fe_{0.5/1.0/1.5}$-CMC-SO_3H catalysts in Scheme 1 [For $Zr_{0.5/1.0/3.0}Fe_{0.5/1.0/1.5}$-SA-$SO_3H$ and $Zr_{1.0}Fe_{0.5/1.0/1.5}$-CMC-SO_3H, the Zr subscript of 0.5/1.0/3.0 meant $ZrOCl_2$ solution concentrations, and the Fe subscript of 0.5/1.0/1.5 meant $Fe_2(SO_4)_3$ solution concentrations].

2.3. Characterization of catalysts

Sulfonated magnetic solid acid ZrFe-SA-SO_3H and ZrFe-CMC-SO_3H were analyzed by various techniques. Their crystal phase was determined by X-ray diffraction (XRD; Rigaku Rotaflex RAD-C, Tokyo, Japan) using CuKα radiation (40 kv and 200 mA). Iron and zirconium contents in catalysts were detected by an inductively coupled plasma-optical emission spectrometer (ICP-OES; Optima 5300, PerkinElmer Inc., Waltham, MA, USA) after catalyst calcination and digestion by acid solution. Fourier transform-infrared spectra (FT-IR) of catalysts were obtained on a Nicolet is10 spectrometer (Thermo Fisher Scientific Co. Ltd., Waltham, MA, USA) over the wavenumber range from 400 to 4000 cm^{-1} with a resolution of 4 cm^{-1}, using the standard KBr disc method. Organic elemental compositions were analyzed by an element analyzer (Vario EL III CHONS, Elementar Analysensysteme GmbH, Hanau, Germany). The morphology and element contents on their surface were detected by scanning electron microscope-X-ray energy dispersive analysis (SEM-EDX) (JSM-IT300, JEOL Ltd., Akishima, Tokyo, Japan). Magnified images of samples were obtained with transmission electron microscope (TEM)(JEM-1200EX, JEOL, Tokyo, Japan). The surface area, pore volume, and pore size were determined by the Bruner-Emmett-Teller (BET) method (Tristar II 3020, Micromeritics Instrument Co., Ltd., Northcross, GA, USA) with N_2 adsorption. Surface acid contents of catalysts (excluding Lewis acid

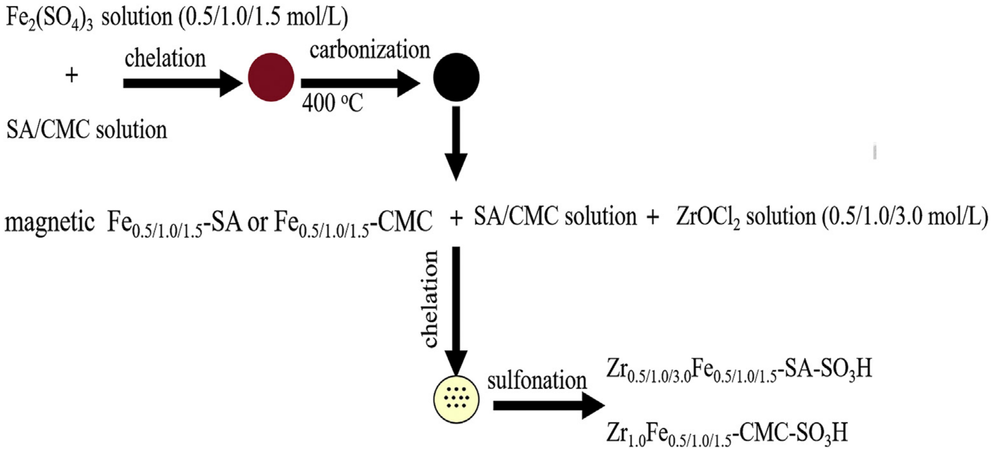

Scheme 1. The preparation of ZrFe-SA/CMC-SO_3H catalysts.

content) were determined by the Boehm titration method [30]. Magnetization of the catalyst was measured by a vibrating sample magnetometer (VSM; lakeshore 7407, Lake Shore Cryotronics, Inc., Westerville, OH, USA). Catalyst thermogravimetric analysis (TG-DSC; STA449F3, NETZSCH-Gerätebau GmbH, Selb, Germany) was conducted with a temperature range from room temperature to 1000 °C and a heating rate of 5 °C/min.

2.4. Oleic acid esterification and product analysis

Oleic acid (0.01 mol), dehydrated methanol (methanol to oleic acid molar ratio of 6/1–18/1) and catalyst (3-11 wt%, relative to oleic acid weight) were mixed in a 50 mL glass bottle sealed by rubber-aluminum cap, and reacted with magnetic stirring in oil bath at 60–100 °C for 2–6 h. After esterification reaction, magnetic catalyst was separated from products by a NdFeB (Ø37 mm × H18 mm) magnet without washing for next reuse. After 5 cycles, catalyst was washed by ethanol to remove residual FAMEs and methanol, and to be calculated the recovery rate of catalyst, which was defined as:

$$\text{Recovery rate(wt\%)} = \text{Weight of recovered catalyst}/\text{Weight of fresh catalyst} \times 100\% \qquad (1)$$

Crude FAMEs at the middle layer of mixed esterification products was drawn out, filtered with organic filter head (pore size 0.22 μm), and dried at 75 °C overnight to remove residual methanol and water. All oleic acid esterification experiments were repeated twice and the standard deviation for FAMEs yield was 0.0–3.5%, listed in Tables 2 and 4.

Crude FAMEs were analyzed by gas chromatography (GC; GC-2014, Shimadzu, Kyoto) with a capillary column of Rtx-Wax (30 m × Ø0.25 mm × 0.25 μm) under analytical conditions of detector temperature 280 °C, injector temperature 260 °C, column temperature 220 °C, carrier gas of helium with a flow rate 1 mL/min and split ratio 40/1. Heptadecanoic acid methyl ester (HAME, $C_{17:\,0}$) as internal standard was used for determining weight of crude FAMEs from GC peaks to calculate FAMEs yield (weight from all GC peaks/actual weight of crude FAMEs × 100%, wt%). Each GC peak was separately calibrated in previous work [31,32] according to the relative response factors [1.023, 1.076, 1.038 and 1.019 for palmitoleate ($C_{16:\,1}$), stearate ($C_{18:\,0}$), oleate ($C_{18:\,1}$) and linoleate ($C_{18:\,2}$) to that of HAME, respectively].

3. Results and discussion

The synthesized sulfonated magnetic solid acid catalysts were characterized by BET, elemental analysis, ICP-OES, Boehm titration, FT-IR, SEM-EDX, TEM, XRD, VSM and TG-DSC to learn their properties with results listed in Table 1, Table 3 and Figs. 1–5, and were tested in the esterification of oleic acid to detect their catalytic activity and stability (Tables 2 and 4).

3.1. Catalyst characterization

3.1.1. BET surface area

The results from the BET surface area for catalysts were listed in Table 1. The concentrations of Zr^{4+} and Fe^{3+} ions during catalyst preparation had a significant influence on the BET surface area and average pore size of catalysts. With the increase of Fe^{3+} and Zr^{4+}

Table 1
BET surface area, pore size, acid content and magnetization for different catalysts.

Catalysts	BET surface area (m^2/g)	Pore size (nm)	Acid content (mmol/g)		Magnetization (Am^2/kg)
			By S content	By NaOH titration	
$Zr_{1.0}Fe_{0.5}$-SA-SO_3H	33.0	18.0	1.92	5.88	6.6
$Zr_{1.0}Fe_{1.0}$-SA-SO_3H	14.3	98.4	1.71	8.39	6.3
After 5 cycle[a]	–	–	1.39	6.75	–
$Zr_{1.0}Fe_{1.5}$-SA-SO_3H	62.2	6.1	2.08	6.38	3.7
$Zr_{0.5}Fe_{1.0}$-SA-SO_3H	48.5	12.0	1.59	5.38	8.1
$Zr_{3.0}Fe_{1.0}$-SA-SO_3H	21.4	187.6	1.61	4.37	5.8
$Zr_{1.0}Fe_{1.0}$-SA-SO_3H (75)	2.3	–	1.39	–	–
Magnetic $Fe_{1.0}$-SA	–	–	–	–	17.8
$Zr_{1.0}Fe_{1.0}$-CMC-SO_3H	–	–	–	–	3.1

[a] Esterification conditions: oleic acid, temperature of 90 °C, time of 4 h, methanol/oleic acid ratio of 12/1 and catalyst amount of 9 wt%.

Table 2
The activity of catalysts for the esterification of oleic acid.

Catalysts	FAMEs yield for every catalyst cycle (wt%)[a]					Catalyst recovery rate (%)[b]
	1	2	3	4	5	
$Zr_{1.0}Fe_{0.5}$-SA-SO_3H	93.2 ± 0.6	92.3 ± 0.3	80.9 ± 0.4	74.4 ± 1.0	63.4 ± 0.1	87.5
$Zr_{1.0}Fe_{1.0}$-SA-SO_3H	94.3 ± 0.7	90.2 ± 0.2	90.3 ± 0.2	88.4 ± 0.2	86.2 ± 3.5	83.6
$Zr_{1.0}Fe_{1.5}$-SA-SO_3H	99.5 ± 0.7	91.6 ± 0.3	81.6 ± 0.8	79.3 ± 1.6	72.2 ± 0.6	85.8
$Zr_{0.5}Fe_{1.0}$-SA-SO_3H	92.7 ± 0.2	90.9 ± 0.9	86.5 ± 2.1	81.5 ± 0.4	78.0 ± 0.4	89.8
$Zr_{3.0}Fe_{1.0}$-SA-SO_3H	94.4 ± 0.6	93.4 ± 0.2	94.3 ± 0.2	84.5 ± 0.1	81.3 ± 0.5	81.6
$Zr_{1.0}Fe_{1.0}$-SA-SO_3H (75)	34.5 ± 3.5	–	–	–	–	–
magnetic $Fe_{1.0}$-SA	61.2 ± 1.7[c]	–	–	–	–	–
$Zr_{1.0}Fe_{0.5}$-CMC-SO_3H	96.7 ± 0.2	90.2 ± 0.1	86.3 ± 2.4	76.2 ± 0.3	64.0 ± 1.2	89.6
$Zr_{1.0}Fe_{1.0}$-CMC-SO_3H	94.2 ± 0.1	91.6 ± 0.8	91.1 ± 0.1	89.3 ± 0.3	85.4 ± 2.5	89.5
$Zr_{1.0}Fe_{1.5}$-CMC-SO_3H	99.8 ± 0.0	83.8 ± 0.8	77.2 ± 0.7	62.9 ± 0.3	60.9 ± 1.9	74.9

[a] Esterification conditions: temperature of 90 °C, time of 4 h, methanol/oleic acid ratio of 12/1 and catalyst amount of 9 wt%. The recovered catalysts were not washed with ethanol before the next cycle.
[b] Error of catalyst recovery rate was less than 0.03%.
[c] Esterification conditions: temperature of 90 °C, time of 5.5 h, methanol/oleic acid ratio of 12/1 and catalyst amount of 9 wt%.

Table 3
Elemental compositions of catalysts analyzed by an elemental analyzer, ICP, and EDX.

Catalysts	Elemental Composition (wt%)							Atomic Ratio[c]	
	N	C	H	S	Zr	Fe	O	S/C	Fe/C
$Zr_{1.0}Fe_{0.5}$-SA-SO_3H	0.05 ± 0.01	47.13 ± 0.06	2.22 ± 0.01	6.17 ± 0.00	0.25	12.82	-[a]	0.049	0.058
After 5 cycles	0.07 ± 0.00	48.47 ± 0.04	2.76 ± 0.07	4.96 ± 0.01	-[a]	-[a]	-[a]	0.038	–
$Zr_{1.0}Fe_{1.0}$-SA-SO_3H	0.03 ± 0.00	43.20 ± 0.28	2.06 ± 0.00	5.49 ± 0.01	0.21	18.80	-[a]	0.048	0.094
	0[b]	56.83[b]	-[a]	3.45[b]	0[b]	9.95[b]	30.76[b]	0.023[b]	0.038[b]
After 5 cycles	0.03 ± 0.01	45.73 ± 0.16	2.61 ± 0.01	4.45 ± 0.02	0.50	13.44	-[a]	0.036	0.063
	0[b]	59.47[b]	-[a]	3.18[b]	0[b]	12.65[b]	23.73[b]	0.020[b]	0.046[b]
$Zr_{1.0}Fe_{1.5}$-SA-SO_3H	0.03 ± 0.00	49.80 ± 0.28	2.29 ± 0.01	6.67 ± 0.12	0.32	7.44	-[a]	0.050	0.032
After 5 cycles	0.03 ± 0.02	52.00 ± 0.06	2.38 ± 0.09	4.86 ± 0.02	-[a]	-[a]	-[a]	0.035	–
$Zr_{0.5}Fe_{1.0}$-SA-SO_3H	0.03 ± 0.00	46.12 ± 0.01	2.25 ± 0.00	5.09 ± 0.04	0.38	12.27	-[a]	0.041	0.057
$Zr_{3.0}Fe_{1.0}$-SA-SO_3H	0.06 ± 0.01	47.31 ± 0.10	2.35 ± 0.03	5.15 ± 0.00	0.70	9.85	-[a]	0.041	0.045
$Zr_{1.0}Fe_{1.0}$-SA-SO_3H (75)	0.05 ± 0.01	39.88 ± 0.06	1.96 ± 0.01	4.45 ± 0.04	-[a]	-[a]	-[a]	0.042	–

[a] The detection was not performed.
[b] Analyzed by EDX, average value of five SEM districts in Fig. 2A (b) for fresh $Zr_{1.0}Fe_{1.0}$-SA-SO_3H and in Fig. 2B (b) for the recovered catalyst after five cycles.

Table 4
Single-factor experiments of oleic acid esterification over fresh $Zr_{1.0}Fe_{1.0}$-SA-SO_3H catalyst.

Temperature (°C)	Methanol/oleic acid molar ratio	Catalyst (wt%)	Time (h)	Biodiesel yield (wt%)
(a)				
60	12	5	4	86.3 ± 0.5
70	12	5	4	89.8 ± 1.2
80	12	5	4	91.6 ± 0.1
90	12	5	4	92.5 ± 0.3
100	12	5	4	92.0 ± 0.7
	(b)			
90	6	5	4	87.0 ± 0.6
90	9	5	4	89.6 ± 1.3
90	12	5	4	92.5 ± 0.3
90	15	5	4	91.7 ± 0.8
90	18	5	4	90.2 ± 1.1
		(c)		
90	12	3	4	83.9 ± 0.4
90	12	5	4	92.5 ± 0.3
90	12	7	4	93.7 ± 1.2
90	12	9	4	94.3 ± 0.7
90	12	11	4	93.8 ± 0.1
			(d)	
90	12	9	2	88.7 ± 1.1
90	12	9	3	93.1 ± 0.9
90	12	9	4	94.3 ± 0.7
90	12	9	5	96.6 ± 0.6
90	12	9	6	96.9 ± 0.4

concentration, the BET surface area of catalysts first decreased and then increased since ion concentration affected the process of chelation. An Fe^{3+} concentration of 0.5 or 1.5 mol/L and a Zr^{4+} concentration of 0.5 or 3.0 mol/L formed a large surface area. Due to the number of binding sites per molecule of SA or CMC for Fe^{3+}or $Zr^{4+}$was limited, therefore varied structure was produced during Na ions in SA or CMC (concentration of 20 g/L) exchanged with Fe ions [$Fe_2(SO_4)_3$ solution with concentrations of 0.5, 1.0, and 1.5 mol/

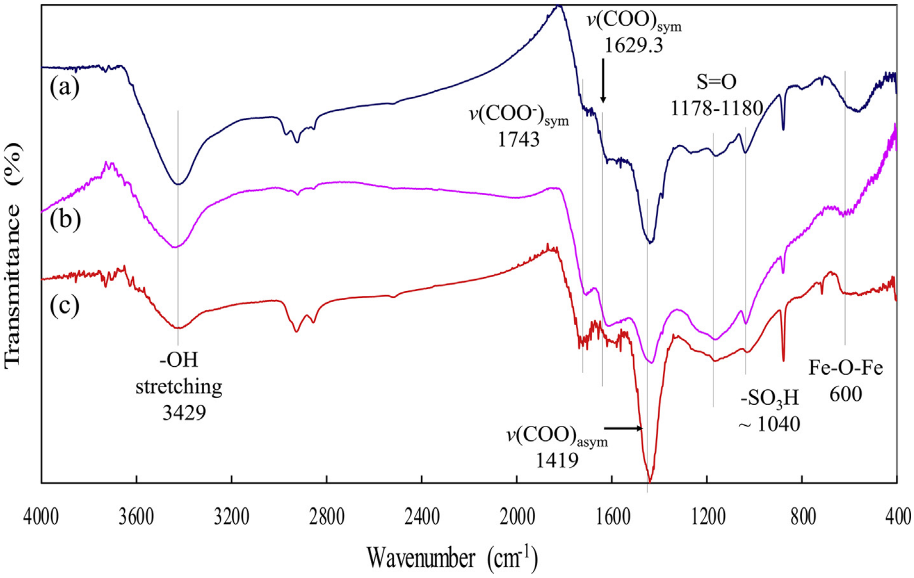

Fig. 1. FT-IR spectra of $Zr_{1.0}Fe_{1.0}$-SA-SO_3H (75) (a), $Zr_{1.0}Fe_{1.0}$-SA-SO_3H (b), and recovered $Zr_{1.0}Fe_{1.0}$-SA-SO_3H catalyst after five cycles (c).

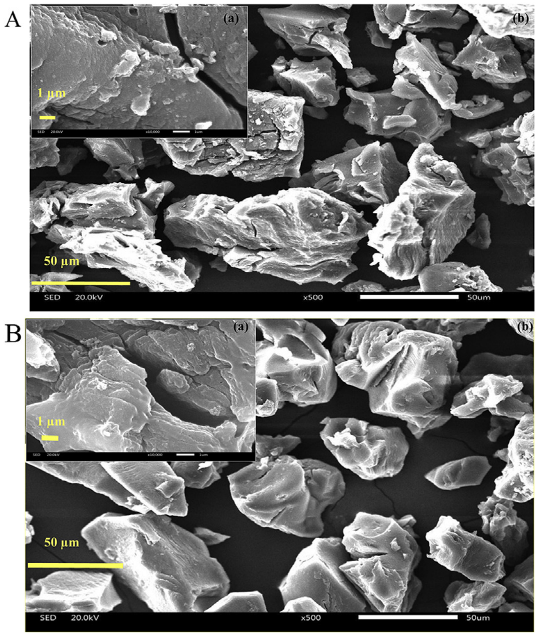

Fig. 2. SEM images of fresh $Zr_{1.0}Fe_{1.0}$-SA-SO_3H catalyst (A) and recovered catalyst after five cycles (B).

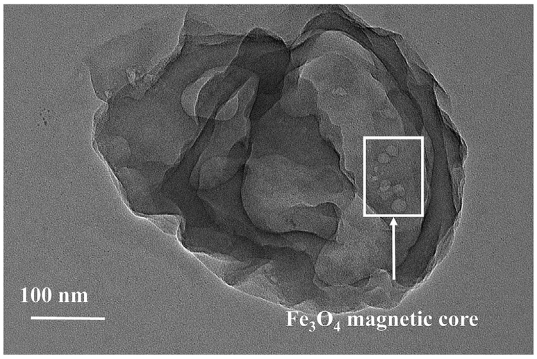

Fig. 3. Transmission electron microscopy spectrum of $Zr_{1.0}Fe_{1.0}$-SA-SO_3H catalyst.

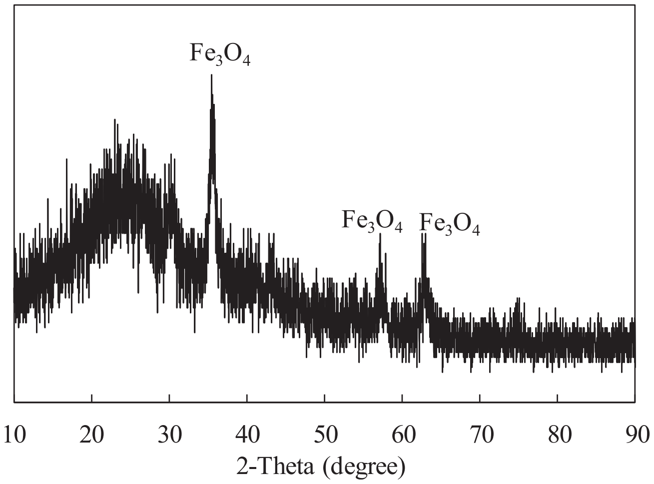

Fig. 4. XRD pattern of $Zr_{1.0}Fe_{1.0}$-SA-SO_3H catalyst.

L] or Zr ions ($ZrOCl_2$ solution with concentrations of 0.5, 1.0, and 3.0 mol/L) [33]. $Zr_{1.0}Fe_{1.5}$-SA-SO_3H with the highest BET surface area (62.2 m^2/g) and moderate pore size (6.1 nm vs. ~1.1 nm for the molecule size of oleic acid) provided the highest esterification activity with a FAMEs yield of 99.5% (Table 2), while $Zr_{1.0}Fe_{1.0}$-SA-SO_3H (75) with a magnetic core particle size of <75 µm provided the lowest BET surface area (2.3 m^2/g) and the worst esterification activity with a FAMEs yield of 34.5%. There was no obvious relationship between catalysts activity and their BET surface area and pore size. However, catalysts with large surface area seemed easy to inactivate, possibly due to the easier blocking or loss of acid sites during the reactions. As a result, the stability of $Zr_{1.0}Fe_{1.5}$-SA-SO_3H (biodiesel yields declined from 99.5 to 72.2% after 5 cycles) was quickly decreased, while $Zr_{1.0}Fe_{1.0}$-SA-SO_3H (biodiesel yields slightly decreased from 94.3 to 86.2% after 5 cycles) with a relatively lower BET surface area could be used for more times based on strong links of sulfonic acid groups.

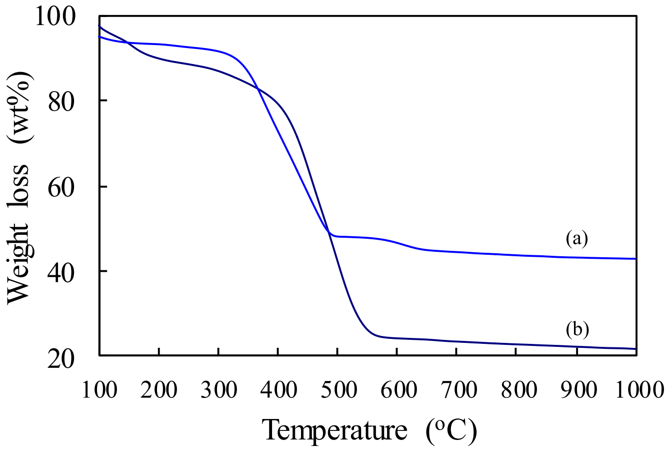

Fig. 5. Thermal stability of magnetic $Fe_{1.0}$-SA (a) and $Zr_{1.0}Fe_{1.0}$-SA-SO_3H catalyst (b).

3.1.2. *Elemental composition*

The elemental compositions of ZrFe-SA-SO_3H catalysts were determined by an elemental analyzer, ICP, and EDX, with the results listed in Table 3. For $Zr_{1.0}Fe_{1.0}$-SA-SO_3H catalyst, the elemental compositions on the catalyst surface and in bulk phase were conducted by EDX, ICP and elemental analyzer. It demonstrated that the catalyst surface contained more C, less S and Fe which indicated sulfonic acid groups and a magnetic core mainly distributed inside the catalyst. The -$(COO)_4Zr$ structure on the surface was very stable and could protect the magnetic core from being dissolved by concentrated sulfuric acid [34], while the -$(COO)_3Fe$ structure was carbonized during the sulfonation process.

After five catalytic cycles, S content on the catalyst surface slightly decreased from 3.45% to 3.18% due to the loss of sulfonic groups during reactions. However, the contents of C and Fe increased from 56.83% to 9.95%–59.47% and 12.65%, respectively, because of the coverage of active sites by oils and magnetic core exposure under magnetic stirring after five cycles.

3.1.3. *Acid amounts and FT-IR*

Acid amounts of ZrFe-SA-SO_3H catalysts were determined the Boehm titration method, and the sulfonic acid contents were obtained from elemental analysis with the results listed in Table 1. The total acid content was titrated by NaOH solution including many acid groups such as carboxylic and sulfonic groups. A different addition of Fe^{3+} and Zr^{4+} concentration resulted in significantly varied amounts and properties of acid sites of catalysts. Fresh $Zr_{1.0}Fe_{1.5}$-SA-SO_3H catalyst possessed the second highest surface acid amounts analyzed by Boehm titration (6.38 mmol/g) and the highest S atomic ratio conducted by the elemental analyzer (0.050), so it gave the highest esterification yield (99.5%) for the first catalytic cycle. But its stability was poor since the sulfonic acid groups easily fell off (S/C atomic ratio decreased to 0.035 after five cycles). Fresh $Zr_{1.0}Fe_{1.0}$-SA-SO_3H catalyst possessed the highest surface acid amounts (8.39 mmol/g) but a reduced S atomic ratio of 0.048 for fresh vs. 0.036 after five cycles, so it gave the second highest esterification yield (94.3%). When comparing the results from the catalyst cycles in Table 2, we could indicate that the connection of acid groups in the $Zr_{1.0}Fe_{1.0}$-SA-SO_3H catalyst was a chemical combination rather than physical adsorption. The surface acid amount of the $Zr_{1.0}Fe_{1.0}$-SA-SO_3H catalyst was much higher than the acid amount calculated by S content (1.71 mmol/g), which demonstrated that the catalyst surface was covered mainly with other acidic groups, such as −COOH, −COO−C, −CO−, and C_6H_5−OH and $-SO_3H$ groups. The reduction of surface acid amounts of ZrFe-SA-SO_3H catalysts was positively correlated with the loss of catalyst activity. After five cycles, 80.5% of surface acid amount and 81.3% of S content still remained for the $Zr_{1.0}Fe_{1.0}$-SA-SO_3H catalyst, which resulted in the slight decrease of the biodiesel yield.

The FT-IR spectra of ZrFe-SA-SO_3H catalysts are shown in Fig. 1. ZrFe-SA-SO_3H catalysts exhibited absorptions for −OH at ~3429 cm^{-1}, for symmetric stretching of COO^- at ~1743 and ~1629.3 cm^{-1} and for asymmetric stretching of COO^- at ~1419 cm^{-1}, which could be attributed to the formation of -$(COO)_3Fe$ and -$(COO)_4Zr$ [35–37]. The bands at 1178–1180 and 1267–1270 cm^{-1} belonged to the stretching of S=O in SO_3H on the surface of sulfonated carbons [38–40], while the bands at ~1040 cm^{-1} referred to the characteristic of $-SO_3H$ [24], all of which confirmed the success of sulfonation on the catalyst surface. The bands at 1178–1180 and ~1040 cm^{-1} seemed significantly decreased on the $Zr_{1.0}Fe_{1.0}$-SA-SO_3H catalyst after five catalytic cycles in Fig. 1c, which demonstrated the loss of sulfonic acid groups during the esterification reactions. The characteristic band of Fe−*O*−Fe stretching was found at around 600 cm^{-1} for Fe_3O_4 [3].

3.1.4. *Electron microscopy, XRD, VSM and TG-DSC*

The SEM images of fresh and recovered $Zr_{1.0}Fe_{1.0}$-SA-SO_3H catalyst after five cycles were presented in Fig. 2, while the TEM image of fresh catalyst was shown in Fig. 3. Fresh catalyst had irregular shapes and apparent carbon stacking on its surface, with a particle size of about 20–70 μm, while after five catalytic cycles, the catalyst surface seemed smoother, possibly due to the physical friction during the reactions. When comparing the TEM image of the fresh $Zr_{1.0}Fe_{1.0}$-SA-SO_3H catalyst in Fig. 3, a nanostructure was found with nano Fe_3O_4 (less than 20 nm) well wrapped within the Zr^{4+} chelated carbon shell. The reason why its particle size analyzed by SEM was bigger than TEM was because the catalyst gathered together with an increase in the storage time due to the magnetic cores (Fe_3O_4) being attracted to each other.

The XRD pattern of fresh $Zr_{1.0}Fe_{1.0}$-SA-SO_3H catalyst was presented in Fig. 4. Only three peaks from Fe_3O_4 in the range of 2θ at 35 and 55–65° were observed, as well as an amorphous feature of the carbon shell at the outside of the catalyst, which was formed by the reduction of the -$(COO)_3Fe$ structure at 400 °C. From Table 1, after embedding and chelation with SA and Zr^{4+} and subsequent sulfonation by concentrated H_2SO_4, the magnetization of fresh ZrFe-SA-SO_3H catalysts was 3.7–8.1 Am^2/kg, which was much lower than the magnetization of magnetic $Fe_{1.0}$-SA (17.8 Am^2/kg). However, it was enough for recovering catalysts from product mixtures with less weight loss. The increase in the ratio of Fe^{3+} and Zr^{4+} ions to SA during catalyst preparation seemed to be of no help to the improvement of catalyst magnetization.

The thermogravimetry curve of fresh $Zr_{1.0}Fe_{1.0}$-SA-SO_3H catalyst was presented in Fig. 5. Compared to magnetic core magnetic $Fe_{1.0}$-SA, $Zr_{1.0}Fe_{1.0}$-SA-SO_3H catalyst showed greater weight loss in the temperature range of 150–600 °C. Two distinct stages at the temperature of 150–350 °C and 350–560 °C were observed, which can possibly be attributed to the instability of the sulfonated surface of the catalyst and the destruction of the magnetic core at a high calcination temperature, respectively.

3.2. *Esterification of oleic acid over ZrFe-SA/CMC-SO_3H catalysts*

At a temperature of 90 °C for 4.0 h with a 12/1 methanol/oleic acid molar ratio, $Zr_{0.5/1.0/3.0}Fe_{0.5/1.0/1.5}$-SA-$SO_3H$ catalysts (9 wt%) were used in the esterification of oleic acid (Table 2). For all $Zr_{0.5/1.0/3.0}Fe_{0.5/1.0/1.5}$-SA-$SO_3H$ catalysts with the size of magnetic $Fe_{1.0}$-SA magnetic core of <425 μm, high FAMEs yields of 92.7–99.5% were obtained for the first cycle (Lines 1–5, Table 2), while $Zr_{1.0}Fe_{1.5}$-SA-

SO_3H gave the highest yield due to its high S content. However, varied stability was observed for these five catalysts with different concentrations of Zr^{4+} and Fe^{3+} ions during catalyst preparation. $Zr_{1.0}Fe_{1.0}$-SA-SO_3H exhibited the best reusability, with a FAMEs yield of 86.2% still being achieved after five catalytic cycles. The concentrations of Fe^{3+} ions during catalyst preparation had the greatest influence on the reuse of the catalyst (magnetization and cyclic activity). After five cycles, FAMEs yields over $Zr_{1.0}Fe_{0.5}$-SA-SO_3H and $Zr_{1.0}Fe_{1.5}$-SA-SO_3H catalysts decreased to 63.4% and 72.7%, respectively. Obviously, a too high or low Fe^{3+} ions concentration was not conducive to improving the stability of the catalyst based on limited binding sites of SA for Fe^{3+} [33]. For $Zr_{0.5}Fe_{1.0}$-SA-SO_3H and $Zr_{3.0}Fe_{1.0}$-SA-SO_3H catalysts, FAMEs yields decreased to 78.0% and 81.3% after five cycles, respectively, which could infer that the concentrations of Zr^{4+} ions had a minor effect on their activities. The concentrations of Zr^{4+} and Fe^{3+} ions showed less influence on the recovery of catalysts due to their strong enough magnetization. However, we found that the FAMEs yield decreased dramatically from 94.3% to 34.5% when the embedding of Zr^{4+} and sulfonation were performed on magnetic $Fe_{1.0}$-SA particles with a size of less than 75 μm because it could not provide enough positions for linking the sulfonic acid groups. Magnetic $Fe_{1.0}$-SA particles also exhibited esterification activity, which produced a FAMEs yield of 61.2% after a 5.5 h reaction based on Lewis acid sites from an unreduced -$(COO)_3Fe$ structure.

A similar situation was observed for ZrFe-CMC-SO_3H catalysts. Three catalysts of $Zr_{1.0}Fe_{0.5}$-CMC-SO_3H, $Zr_{1.0}Fe_{1.0}$-CMC-SO_3H, and $Zr_{1.0}Fe_{1.5}$-CMC-SO_3H produced FAMEs yields of 94.2–99.8% for the first cycle, while the stability of catalysts exhibited a significant difference (Lines 8–10, Table 2). $Zr_{1.0}Fe_{1.0}$-CMC-SO_3H can be continuously used for five cycles, with a FAMEs yield of higher than 85.4%, but the FAMEs yields after five cycles decreased to 64.0% and 60.9% over $Zr_{1.0}Fe_{0.5}$-CMC-SO_3H and $Zr_{1.0}Fe_{1.5}$-CMC-SO_3H, respectively.

In summary, catalysts of $Zr_{1.0}Fe_{1.0}$-CMC-SO_3H and $Zr_{1.0}Fe_{1.0}$-SA-SO_3H showed excellent catalytic activity for biodiesel production *via* esterification, but only $Zr_{1.0}Fe_{1.0}$-SA-SO_3H was selected as the suitable one because of (i) its high magnetization of 6.3 Am^2/kg compared with a magnetization of 3.1 Am^2/kg from $Zr_{1.0}Fe_{1.0}$-CMC-SO_3H, which could ensure a high recovery rate for the catalyst cycle in the sustainable biodiesel production for industrial applications, and (ii) its high catalyst yield for $Zr_{1.0}Fe_{1.0}$-SA-SO_3H (more quality of catalyst can be obtained when the same mass of raw materials were added during catalyst preparation).

3.3. Single-factor experiments of oleic acid esterification over $Zr_{1.0}Fe_{1.0}$-SA-SO_3H catalyst

The selected catalyst $Zr_{1.0}Fe_{1.0}$-SA-SO_3H was used for biodiesel production by the esterification of oleic acid. Reaction conditions of temperature, methanol/oleic acid molar ratio, catalyst dosage, and reaction time were studied, and the results were listed in Table 4.

Under conditions of a methanol/oleic acid molar ratio of 12/1, catalyst of 5 wt%, and a time of 4 h, the biodiesel yield increased from 86.3% to 92.5% as the temperature grew from 60 to 90 °C, as shown in Table 4a. When the reaction temperature increased to 100 °C, the yield of biodiesel decreased to 92.0%. So, the best temperature was chosen as 90 °C.

The influence of the methanol/oleic acid molar ratio was conducted under reaction conditions of 90 °C, 5 wt% catalyst, and 4 h in Table 4b. The yield of biodiesel first grew to the maximum value of 92.5% and decreased to 90.2% with a methanol/oleic acid molar ratio that changed from 9/1 to 18/1. Excess methanol was disadvantageous for the catalyst thoroughly mixed in oleic acid and methanol [32]. Therefore, methanol/oleic acid molar ratio of 12/1 was selected.

Under conditions of 90 °C, 12/1 methanol/oleic acid ratio, and 4 h, the effect of catalyst dosage was studied in Table 4c. As the weight of the catalyst added in the reaction increased from 3 to 9 wt%, the biodiesel yield achieved its maximum value of 94.3%, but it declined to 93.8% when the catalyst dosage continued to grow to 11 wt%. Obviously, excess catalyst added was not beneficial for stirring the reactants well. Hence, a catalyst dosage of 9 wt% with the highest product yield of 94.3% was selected as the best value for the next investigation.

The impact of reaction time was conducted at 90 °C, a 12/1 methanol/oleic acid ratio, and 9 wt%. The biodiesel yield increased to 96.6% at 5 h in Table 4d, and it changed a little when the time was prolonged from 5 to 6 h. So, a time of 5 h was most suitable.

In conclusion, the suitable conditions with a biodiesel yield of 96.6% for oleic acid esterification over the $Zr_{1.0}Fe_{1.0}$-SA-SO_3H catalyst were a reaction temperature of 90 °C, methanol/oleic acid molar ratio of 12/1, 9 wt% catalyst, and reaction time of 5 h. The conditions were moderate compared with the results of 100 °C for 10 h for the reported H_2SO_4–Zr_2O catalyst [40]. These optimal conditions were used in the following catalyst cycle.

3.4. Catalyst cycle under optimal conditions

The recovered $Zr_{1.0}Fe_{1.0}$-SA-SO_3H catalyst was reused for the esterification of oleic acid under the optimized conditions of 90 °C for 5 h, a methanol/oleic acid molar ratio of 12/1, and 9 wt% catalyst. Biodiesel yield declined from 96.6% to 90.3% after five cycles without ethanol washing for each cycle with an 81.3% recovery rate. The specific activity of the catalyst (activity per unit mass of catalyst) was higher than that of the fresh catalyst because the residual high purity biodiesel in reaction bottle slightly increased biodiesel yield. According to the results from NaOH titration and elemental analysis in Tables 1 and 3, the total acid content and S/C atomic ratio of recovered $Zr_{1.0}Fe_{1.0}$-SA-SO_3H catalyst decreased from 8.30 to 6.75 mmol/g (from 0.048 to 0.036 for S/C atomic ratio) which also implied that the acidic site lose slightly. Solid acid catalysts, such as acidic carbonaceous catalyst E-P400-2-SO_3H [24] with no magnetization esterified oleic acid at 80 °C for 5 h with biodiesel yields of 95.5%, 90.2%, 84.6%, 68.3%, and 47% for five cycles, and Cs-tungstosilicic acid catalyzed oleic acid esterification at 120 °C within 5 h obtaining biodiesel yields of 88%, 79%, 67%, 60% and 49% for five cycles [25], were reported. So, $Zr_{1.0}Fe_{1.0}$-SA-SO_3H catalyst synthesized in this work showed an excellent cycle capability for application.

4. Conclusions

Biodiesel production was catalyzed by sulfonated magnetic solid acid catalysts (ZrFe-SA-SO_3H) with a high acid content (4.4–8.4 mmol/g) synthesized through four steps: (1) chelation with SA and Fe^{3+}; (2) calcination; (3) chelation and embedding with SA and Zr^{4+}; and (4) sulfonation. The prepared catalysts showed considerable activity for biodiesel production (92.7–99.5%) from the esterification of oleic acid. However, only catalyst $Zr_{1.0}Fe_{1.0}$-SA-SO_3H with a proper embedding ratio of Fe and Zr elements showed the best reusability of the catalyst. A high biodiesel yield of 90.3% was still achieved after five cycles of $Zr_{1.0}Fe_{1.0}$-SA-SO_3H. A similar situation was also observed when using CMC to replace SA during catalyst preparation.

Acknowledgements

The authors wish to acknowledge the financial support from Chinese Academy of Sciences [CAS 135 program (XTBG-T02) and equipment R&D grant (No.YZ201260)], the Natural Science Foundation of China (No. 31400518). The authors thank to Professor Zhen Fang from Nanjing Agricultural University for his valuable advices. Thanks are also given to Doctor Fan Zhang and Miss Wenjing Yang from Xishuangbanna Tropical Botanical Garden (XTBG), and to the Central Laboratory of XTBG.

References

[1] J.F. Costa, M.F. Almeida, M.C.M. Alvim-Ferraz, J.M. Dias, Biodiesel production using oil from fish canning industry wastes, Energy Convers. Manag. 74 (2013) 17–23.

[2] J. Dupont, P.A.Z. Suarez, M.R. Meneghetti, S.M.P. Meneghetti, Catalytic production of biodiesel and diesel-like hydrocarbons from triglycerides, Energy Environ. Sci. 2 (2009) 1258–1265.

[3] Zillillah, G.W. Tana, Z. Li, Highly active, stable, and recyclable magnetic nanosize solid acid catalysts: efficient esterification of free fatty acid in grease to produce biodiesel, Green Chem. 14 (2012) 3077–3086.

[4] L.T. Thanh, K. Okitsu, Y. Sadanaga, N. Takenaka, Y. Maeda, H. Bandow, Ultrasound assisted production of biodiesel fuel from vegetable oils in a small scale circulation process, Bioresour. Technol. 101 (2010) 639–645.

[5] P.D. Luu, H.T. Truong, B.V. Luu, L.N. Pham, K. Imamura, N. Takenaka, Y. Maeda, Production of biodiesel from Vietnamese *Jatropha curcas* oil by a co-solvent method, Bioresour. Technol. 173 (2014) 309–316.

[6] S. Sankaranarayanan, C.A. Antonyraj, S. Kannan, Transesterification of edible, nonedible and used cooking oils for biodiesel production using calcined layered double hydroxides as reusable base catalysts, Bioresour. Technol. 109 (2012) 57–62.

[7] O. Kaarstad, Fossil fuels and responses to global warming, Energy Convers. Manag. 36 (1995) 869–872.

[8] M.M. Gui, K.T. Lee, S. Bhatia, Feasibility of edible oil *vs.* non-edible oil *vs.* waste edible oil as biodiesel feedstock, Energy 33 (2008) 1646–1653.

[9] M. Hadnadjev-Kostic, T. Vulic, R. Marinkovic-Neducin, D. Loncarevic, J. Dostanic, S. Markov, D. Jovanovi, Photo-induced properties of photocatalysts: a study on the modified structural, optical and textural properties of TiO2-ZnAl layered double hydroxide based materials, J. Clean. Prod. 164 (2017) 1–18.

[10] A. Sivasamy, K.Y. Cheah, P. Fornasiero, F. Kemausuor, S. Zinoviev, S. Miertus, Catalytic applications in the production of biodiesel from vegetable oils, ChemSusChem 2 (2009) 278–300.

[11] D.M. Alonso, J.Q. Bond, J.A. Dumesic, Catalytic conversion of biomass to biofuels, Green Chem. 12 (2010) 1493–1513.

[12] E. Lois, Definition of biodiesel, Fuel 86 (2007) 1212–1213.

[13] T.K. Amin, N.A.S. Amin, H. Mazaheri, A review on novel processes of biodiesel production from waste cooking oil, Appl. Energy 104 (2013) 683–710.

[14] M. Hájek, F. Skopal, L. Čapek, M. Černoch, P. Kutálek, Ethanolysis of rapeseed oil by KOH as homogeneous and as heterogeneous catalyst supported on alumina and CaO, Energy 48 (2012) 392–397.

[15] J.M. Balbino, E.W. de Menezes, E.V. Benvenutti, R. Cataluna, G. Ebeling, J. Dupont, A review on novel processes of biodiesel production from waste cooking oil, Green Chem. 13 (2011) 3111–3116.

[16] M.J. Montefrio, T. Xinwen, J.P. Obbard, Recovery and pre-treatment of fats, oil and grease from grease interceptors for biodiesel production, Appl. Energy 87 (2010) 3155–3161.

[17] R.S. Watkins, A.F. Lee, K. Wilson, Li-CaO catalysed tri-glyceride transesterification for biodiesel applications, Green Chem. 6 (2004) 335–340.

[18] Q.H. Liu, B.C. Wang, C.X. Wang, Z.J. Tian, W. Qu, H.J. Ma, R.S. Xu, Basicities and transesterification activities of Zn-Al hydrotalcites-derived solid bases, Green Chem. 16 (2014) 2604–2613.

[19] A.M. El-Nahas, T.A. Salaheldin, T. Zaki, H.H. El-Maghrabi, A.M. Marie, S.M. Morsy, N.K. Allam, Functionalized cellulose-magnetite nanocomposite catalysts for efficient biodiesel production, Chem. Eng. J. 322 (2017) 167–180.

[20] F. Omota, A.C. Dimian, A. Bliek, Fatty acid esterification by reactive distillation: Part 2-kinetics-based design for sulphated zirconia catalysts, Chem. Eng. Sci. 58 (2003) 3175–3185.

[21] A.A. Kiss, A.C. Dimian, G. Rothenberg, Solid acid catalysts for biodiesel production -towards sustainable energy, Adv. Synth. Catal. 348 (2006) 75–81.

[22] D.E. López, J.G. Goodwin Jr., D.A. Bruce, E. Lotero, Transesterification of triacetin with methanol on solid acid and base catalysts, Appl. Catal. A Gen. 295 (2005) 97–105.

[23] L. Soh, J. Curry, E.J. Beckman, J.B. Zimmerman, Effect of system conditions for biodiesel production via trans-esterification using carbon dioxide-methanol mixtures in the presence of a heterogeneous catalyst, ACS Sustain. Chem. Eng. 2 (2014) 387–395.

[24] M. Huang, J. Luo, Z. Fang, H. Li, Biodiesel production catalyzed by highly acidic carbonaceous catalysts synthesized via carbonizing lignin in sub- and supercritical ethanol, Appl. Catal. B Environ. 190 (2016) 103–114.

[25] S. Gopinath, P. Vinoth Kumar, P. Sahaya Murphin Kumar, K.A. Yasar Arafath, S. Sivanesan, P. Baskaralingam, Cs-tungstosilicic acid/Zr-KIT-6 for esterification of oleic acid and transesterification of non-edible oils for green diesel production, Fuel 234 (2018) 824–835.

[26] V.M. De Aguiar, A.L.F. de Souza, F.S. Galdino, M.M.C. da Silva, V.G. Teixeira, E.R. Lachter, Sulfonated poly (divinylbenzene) and poly (styrene-divinylbenzene) as catalysts for esterification of fatty acids, Renew. Energy 114 (2017) 725–732.

[27] Y. Wang, D. Zhao, G. Chen, S. Liu, N. Ji, H. Ding, J. Fu, Preparation of phosphotungstic acid based poly(ionic liquid) and its application to esterification of palmitic acid, Renew. Energy 133 (2019) 317–324.

[28] K.P. Flores, J.L.O. Omega, L.K. Cabatingan, A.W. Go, R.C. Agapay, Y.H. Ju, Simultaneously carbonized and sulfonated sugarcane bagasse as solid acid catalyst for the esterification of oleic acid with methanol, Renew. Energy 130 (2019) 510–523.

[29] S. Niu, Y. Ning, C. Lu, K. Han, H. Yu, Y. Zhou, Esterification of oleic acid to produce biodiesel catalyzed by sulfonated activated carbon from bamboo, Energy Convers. Manag. 163 (2018) 59–65.

[30] H.P. Boehm, Surface oxides on carbon and their analysis: a critical assessment, Carbon 40 (2002) 145–149.

[31] B.J. Xue, J. Luo, F. Zhang, Z. Fang, Biodiesel production from soybean and *Jatropha* oils by magnetic CaFe$_2$O$_4$-Ca$_2$Fe$_2$O$_5$-based catalyst, Energy 68 (2014) 584–591.

[32] Y.T. Wang, Z. Fang, F. Zhang, B.J. Xue, One-step production of biodiesel from oils with high acid value by activated Mg–Al hydrotalcite nanoparticles, Bioresour. Technol. 193 (2015) 84–89.

[33] K.J. Sreeram, H.Y. Shrivastava, B.U. Nair, Studies on the nature of interaction of iron(III) with alginates, Biochim. Biophys. Acta 1670 (2004) 121–125.

[34] Y.T. Wang, Z. Fang, F. Zhang, Esterification of oleic acid to biodiesel catalyzed by a highly acidic carbonaceous catalyst, Catal. Today 319 (2019) 172–181.

[35] P.L. Boey, S. Ganesan, G.P. Maniam, M. Khairuddean, S.E. Lee, A new heterogeneous acid catalyst system for esterification of free fatty acids into methyl esters, Appl. Catal. A Gen. 433–434 (2012) 12–17.

[36] J. Wang, X.Y. Lin, X.G. Luo, Y.F. Long, A sorbent of carboxymethyl cellulose loaded with zirconium for the removal of fluoride from aqueous solution, Chem. Eng. J. 252 (2014) 415–422.

[37] F.A. Dawodu, O. Ayodele, J.Y. Xin, S.J. Zhang, D.X. Yan, Effective conversion of non-edible oil with high free fatty acid into biodiesel by sulphonated carbon catalyst, Appl. Energy 114 (2014) 819–826.

[38] K. Malins, V. Kampars, J. Brinks, I. Neibolte, R. Murnieks, Synthesis of activated carbon based heterogenous acid catalyst for biodiesel preparation, Appl. Catal. B Environ. 176–177 (2015) 553–558.

[39] L.J. Konwara, P. Mäki-Arvela, E. Salminen, N. Kumar, A.J. Thakur, J. Mikkola, D. Deka, Towards carbon efficient biorefining: multifunctional mesoporous solid acids obtained from biodiesel production wastes for biomass conversion, Appl. Catal. B Environ. 176–177 (2015) 20–35.

[40] Y. Zhang, W.T. Wong, K.F. Yung, Biodiesel production *via* esterification of oleic acid catalyzed by chlorosulfonic acid modified zirconia, Appl. Energy 116 (2014) 191–198.